


RESEARCH ARTICLE

Open Access



# BODIPY dyads and triads: synthesis, optical, electrochemical and transistor properties

Sompit Wanwong<sup>1,2\*</sup> , Piyachai Khomein<sup>3</sup> and S. Thayumanavan<sup>3</sup>

**Abstract:** A series of D–A dyads and D–A–D triads molecular systems based on triphenylamine and 9-ethyl-carbazole as donor (D) and BODIPY as acceptor (A) has been designed and synthesized. The optoelectronic properties including optical, electrochemical, and charge carrier mobility of these molecules have been investigated. We found that the D–A–D triads exhibited broader absorption, raising the HOMO energy levels and increase hole carrier mobilities. Analysis surface morphology revealed that BODIPY containing carbazole demonstrated smooth film and no macro phase aggregation was observed upon thermal annealing.

**Keywords:** Donor–acceptor, Donor–acceptor–donor, BODIPY, Organic semiconductor, Transistor property, Surface morphology

## Introduction

Organic semiconductors are crucial component in organic photovoltaics since they served as both light harvesting unit and charge transporting material that involved in energy conversion process. To effectively convert solar energy into electrical current, the organic semiconductors should have broad and intense absorption to harvest photon flux from the solar spectrum, proper HOMO and LUMO energy levels and sufficient charge carrier mobility to facilitate charge separation process [1, 2]. Typically, organic semiconductors consist of  $\pi$ -conjugated system which can be either small molecules or polymer based aromatic compounds. Polymer based semiconductors offer broader absorption, low cost deposition processing in small and large area [3–5]. However, they are polydisperse and tended to have batch-to-batch variation, higher molecular disorder and impurity from the end groups [6, 7]. In contrast, small  $\pi$ -conjugated molecules provide benefit on high purity with defined chemical structures, precise molecular weight and

synthetically reproducible [6, 7]. These make small molecules gaining more attention to utilize in organic photovoltaics.

Recently, 4,4-difluoro-4-bora-3a,4a-diaza-s-indacen or boron dipyrromethene (BODIPY) has been explored for optoelectronic applications [8–10]. BODIPY is attractive heteroatom building block for organic semiconductor because it possesses excellent absorption properties with high molar absorptivity, high quantum yield and high photo-bleaching life time [11, 12]. The BODIPY core has three locations, the *meso*-position, the pyrrolic positions and the boron atom position, in which  $\pi$ -conjugation substituents can be attached [13, 14]. The effect of BODIPY structures on photophysical properties has been intensively explored [10, 13], while fundamental understanding on relationship between structures and charge transport property is less investigated. Generally, BODIPY based small molecules have been designed using symmetrical D–A–D and A–D–A triads [15, 16], where donor (D) is an electron rich functionality and acceptor (A) is a BODIPY unit. For instances, Krishnamoorthy et al. [17] studied the effect of alkyl side chains at the *meso*-position of triphenylamine-BODIPY-triphenylamine triads on the charge transport properties. The hole mobilities of those BODIPY were found in the range of  $10^{-5}$ – $10^{-7}$  cm<sup>2</sup>/V s. Recently, Thayumanavan

\*Correspondence: sompit.wan@kmutt.ac.th

<sup>1</sup> Polymer for Energy, Environment and Technology Research Group, Division of Materials Technology, School of Energy, Environment and Materials, King Mongkut's University of Technology Thonburi, 126 Pracha Uthit Rd., Bang Mod, Thung Khru, Bangkok 10140, Thailand  
Full list of author information is available at the end of the article

et al. [18] developed the A–D–A structures where various donor moieties were incorporated at the *meso*-position of the BODIPY. They found that insertion of cyclopentadithiophene as the donor unit provided the highest electron mobility in the range of  $10^{-5}$  cm<sup>2</sup>/V s. With the similar triad architecture, Facchetti et al. [19] reported that BODIPY-quaterthiophene-BODIPY can create crystalline fiber, resulting in high electron mobility of  $10^{-2}$  cm<sup>2</sup>/V s. These examples suggest that charge transport characteristic of BODIPY can be either p-type (hole mobility) or n-type (electron mobility), depending on molecular architecture (D–A–D or A–D–A). Moreover, molecular packing of BODIPY is strongly influenced on charge mobility [17, 19].

Considering the variety of molecular systems, the relationship between D–A and D–A–D molecular structures on optical properties, charge mobility and surface morphology are of our interest. To broadening our understanding, we have designed to incorporate two different donor units on the BODIPY core. We chose triphenylamine (TPA) and carbazole (CBZ) as donor functionalities because they were easily oxidized into the radical cation and they have been largely employed in various optoelectronic devices [20, 21]. The donor units were attached at the 2- and 6-positions of the BODIPY acceptor to obtained dyad and triad structures. The substitution at the 2,6-position is expected to provide high degree of planarity and effective conjugation [13, 15]. Here, we described the optical, electrochemical of the BODIPYs, namely, TPA-BODIPY, CBZ-BODIPY, TPA-BODIPY-TPA and CBZ-BODIPY-CBZ, respectively (Fig. 1). The field-effect transistors were fabricated. The transistor properties and surface morphology of BODIPY derivatives have been investigated. The relationship between the resulting morphology and device performance is analyzed.

## Results and discussion

### Synthesis

The target BODIPYs (3–6) were prepared in three steps as depicted in Scheme 1. First, BODIPY precursor was iodination using 1.2 equivalent of *N*-iodosuccinimide (NIS) to give 2-iodo-BODIPY (1) and 2.5 equivalent of NIS to give 2,6-diiodo-BODIPY (2) in good yield. The 2-iodo-BODIPY and the 2,6-diiodo-BODIPY were then incorporated with triphenylamine-4-boronic acid or 9-ethylcarbazole-3-boronic acid using Suzuki–Miyaura cross coupling reaction to yield the corresponding products (3–6), TPA-BODIPY, CBZ-BODIPY, TPA-BODIPY-TPA and CBZ-BODIPY-CBZ, respectively. The chemical structures were characterized using <sup>1</sup>H-NMR, <sup>13</sup>C-NMR and mass spectrometry to confirm their identity and purity (see Additional file 1).

### Absorption properties

The optical properties of BODIPY dyads and triads (concentration of  $10^{-5}$  M) were examined in dichloromethane solution using UV–Vis spectrophotometry. The steady-state absorption spectra of D–A and D–A–D have shown in Fig. 2. The photophysical parameters including absorption maxima, molar extinction coefficient, absorption onset and optical spectra were determined, as shown in Table 1. The BODIPY dyads and triads exhibited two strong absorption bands at 269–307 and at 511–531 nm with the extinction coefficients in the range of  $10^4$  M<sup>-1</sup> cm<sup>-1</sup>. The first absorption band was attributed to the absorption of the donor moieties, triphenylamine and carbazole, whereas the second absorption band was attributed to the intramolecular charge transfer (ICT) from donor to the BODIPY unit. The absorption maxima of TPA-BODIPY-TPA and CBZ-BODIPY-CBZ are red-shifted by 25 nm and 20 nm, comparing to those of TPA-BODIPY and CBZ-BODIPY, respectively. The longer absorption was due to the extended conjugation length of the BODIPY triads. The optical bandgaps were determined from the long wavelength absorption edge ( $\lambda_{\text{onset}}$ ) using the equation  $E_g = 1240/\lambda_{\text{onset}}$ . As a result, the energy bandgap ( $E_g$ ) of TPA-BODIPY, CBZ-BODIPY, TPA-BODIPY-TPA and CBZ-BODIPY-CBZ were 2.05, 2.07, 1.98 and 2.00 eV, respectively. Thus, TPA-BODIPY-TPA exhibited the lowest energy bandgap. This is due to the strong electron donation ability of triphenylamine unit that enhance intramolecular charge transfer to the BODIPY acceptor unit [20, 22].

### Electrochemical properties

The electrochemical properties of BODIPY derivatives were analyzed using cyclic voltammetry. The solution of BODIPYs in anhydrous dichloromethane were prepared and the electrochemical characterization were performed using three-electrode system. The cyclic voltammogram and energy levels are illustrated in Fig. 3. The redox properties, the estimated HOMO and LUMO energy levels are summarized in Table 1. Cyclic voltammograms of all compounds exhibited only reversible oxidation wave. The oxidation potentials of TPA-BODIPY, CBZ-BODIPY, TPA-BODIPY-TPA and CBZ-BODIPY-CBZ were 0.39, 0.45, 0.23, and 0.37 V versus Ag/AgCl, respectively. These corresponded to the HOMO energy levels of –5.03, –5.10, –4.92 and –5.06 eV. Incorporation of triphenylamine units to the BODIPY core provided higher HOMO energy levels, suggesting that triphenylamine is stronger electron donor than carbazole. This is consistent to the longer  $\lambda_{\text{onset}}$  in the optical spectrum (Fig. 2). The LUMO energy levels were estimated using the optical bandgap.

### Charge transport properties

Charge carrier mobility of BODIPY dyads and triads were characterized in thin film using the bottom contact field effect transistor (FET). The charge carrier mobilities were calculated using the following equation [24, 25]:

$$I_D = (\mu C_i W / 2L) [(V_{GS} - V_T)]$$

where  $I_D$  is the current flowing between drain and source gates,  $\mu$  is the mobility,  $C_i$  is the capacitance of the gate dielectric,  $W$  is the channel width,  $L$  is the channel length,  $V_{GS}$  is the gate-source voltage and  $V_T$  is the threshold voltage.

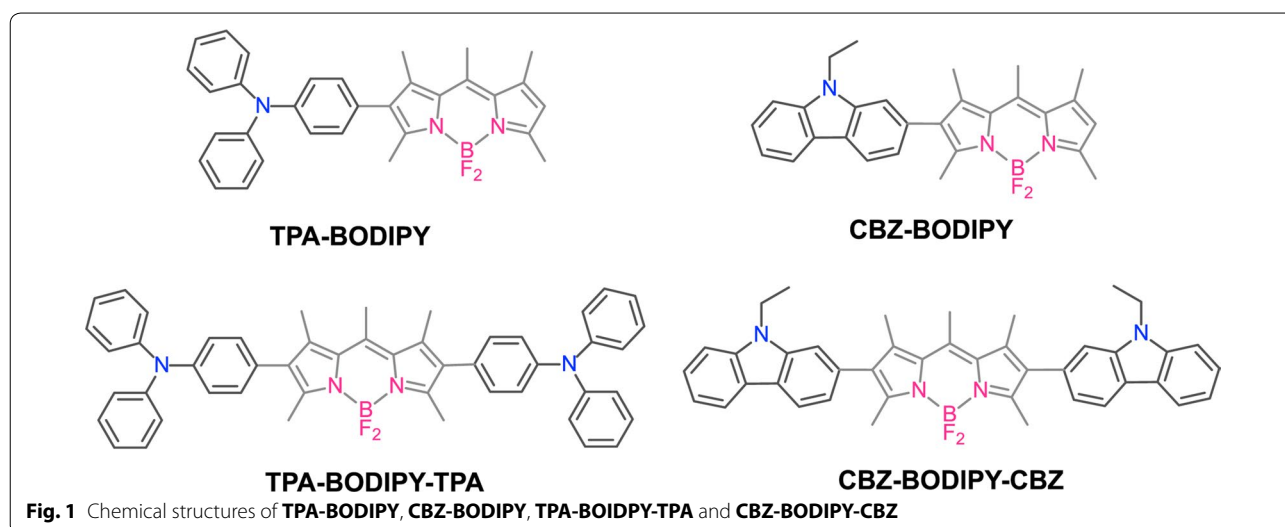
Charge transport characteristic of BODIPY derivatives has been tested for both hole and electron mobility. The measurements were carried in a glovebox under argon atmosphere. The carrier mobility, threshold voltage and on/off current ratio are summarized in Table 2. We found that all compounds demonstrate only hole mobility, thus they behave as p-type semiconductors. For the D–A dyads system, the mobility of **TPA-BODIPY** and **CBZ-BODIPY** were found to be  $9.27 \times 10^{-7}$  and  $5.29 \times 10^{-8}$   $\text{cm}^2/\text{V s}$ , respectively. Increasing conjugation length of D–A–D triads provided higher mobility and increase of on/off current ratio. As seen in Table 2, **TPA-BODIPY-TPA** and **CBZ-BODIPY-CBZ** exhibited mobility of  $1.66 \times 10^{-6}$  and  $7.86 \times 10^{-6}$   $\text{cm}^2/\text{V s}$ , respectively. The increased hole mobility could be correlated to the higher HOMO energy levels of the D–A–D system that facilitate hole charge to travel to the Fermi level of the gold metals. After annealing samples at  $80^\circ\text{C}$  in a glovebox under argon atmosphere for 3 h, the mobilities of BODIPYs were improved by over an order of magnitude. As a result, **CBZ-BODIPY-CBZ** obtained the highest mobility of  $2.95 \times 10^{-5}$   $\text{cm}^2/\text{V s}$  (Fig. 4b). This value is

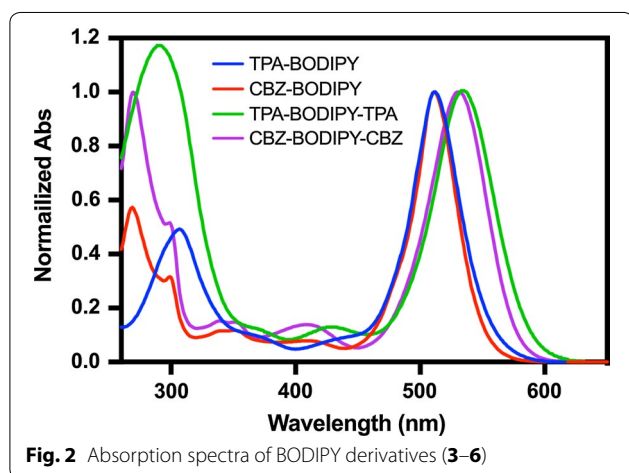
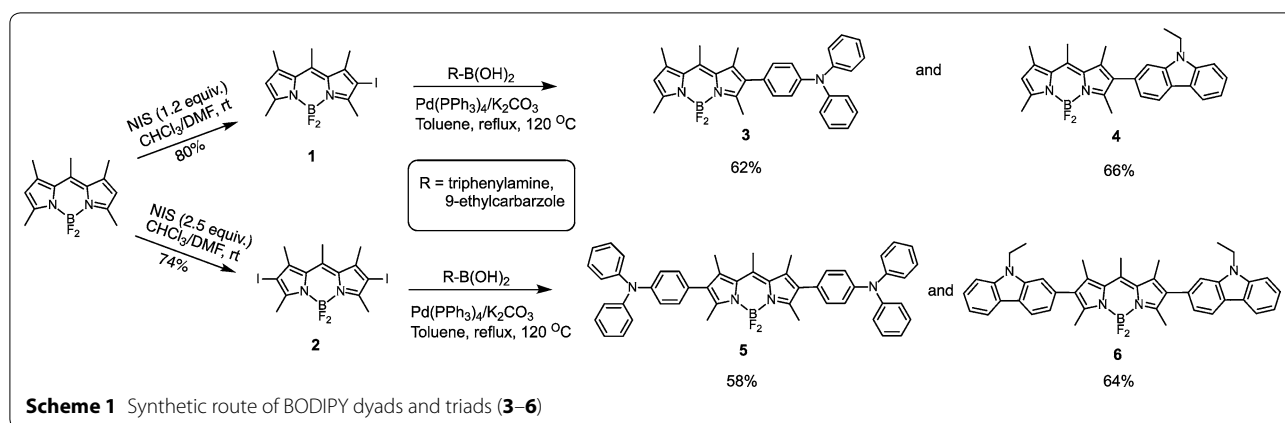
comparable to other reported BODIPY based small molecules that exhibit uniform film [17, 18].

The difference in mobility are usually related to the difference of molecular packing in solid state, film morphology and the structural defects [26–28]. To gain more information, AFM has been conducted in a tapping mode. The **TPA-BODIPY**, **CBZ-BODIPY**, **TPA-BODIPY-TPA** and **CBZ-BODIPY-CBZ** showed completely different film textures (Fig. 5). **TPA-BODIPY** exhibited obvious large grain separation, while **CBZ-BODIPY** showed more homogeneous and smooth morphology with low root mean square of average height (RMS) (0.23 nm). The flatter film of **CBZ-BODIPY** could be attributed to more planarity of carbazole unit, resulting in reduced torsion between the donor and the BODIPY acceptor. For the triad architectures, **TPA-BODIPY-TPA** film showed terrace-like structure and increasing of surface roughness after annealing. This poor film morphology is consistent with deterioration of the hole mobility. On the contrary, **CBZ-BODIPY-CBZ** revealed smooth surface with RMS of 0.18 nm. Decreasing in surface roughness suggests that introduction of ethyl carbazole groups tend to create more uniform film, thus the higher charge carrier mobility could be related to well-organized surface.

### Conclusion

In summary, we have synthesized BODIPY dyads and triads using triphenylamine and carbazole as electron donating groups. The BODIPY triads demonstrated higher hole carrier mobilities, as compared to the BODIPY dyads. FET device containing **CBZ-BODIPY-CBZ** exhibited mobility as high as  $2.95 \times 10^{-5}$   $\text{cm}^2/\text{V s}$ . Although the BODIPY derivatives provided moderate performance, we hope that this work would benefit on





rational design of the next BODIPY semiconductors to optimize their transistor properties.

## Experimental section

### Materials

All reagents were purchased from TCI chemicals, Aldrich and Fisher. Deuterated chloroform ( $\text{CDCl}_3$ ) was purchased from Cambridge Isotope Laboratories. Silica gel for column chromatography was purchased from Silicycle. All chemicals were used as received.

### Synthesis details

#### Synthesis of 2-iodo-BODIPY (**1**)

[[[(3,5-Dimethyl-1*H*-pyrrol-2-yl)(3,5-dimethyl-2*H*-pyrrol-2-ylidene)methyl]methane]-(difluoroborane) or BODIPY (0.5 g, 1.9 mmol) was dissolved in chloroform (20 mL) and the reaction mixture was degassed for 10 min. A solution of *N*-iodosuccinimide (NIS) (0.52 g, 2.3 mmol) in anhydrous DMF (4 mL) was slowly added to a solution mixture. The reaction mixture was stirred at room temperature for 24 h. After that, the crude mixture was extracted with ethyl acetate and water. The organic layers were dried over  $\text{Na}_2\text{SO}_4$  and concentrated using a rotary evaporator. The crude mixture was then purified by column chromatography over silica with DCM/hexane as an eluent to give the product **1** as orange powder (0.6 g, 80%)  $^1\text{H-NMR}$  (500 MHz,  $\text{CDCl}_3$ ):  $\delta$  (ppm), 6.10 (s, 1H,  $\text{CH}_{\text{PYR}}$ ), 2.59 (s, 3H,  $\text{CH}_3$ ), 2.54–2.52 (d, 6H,  $\text{CH}_3$ ), 2.40–2.38 (d, 6H,  $\text{CH}_3$ ) MALDI-TOF MS ( $m/z$ ) calculated for  $\text{C}_{14}\text{H}_{16}\text{BF}_2\text{IN}_2$  [ $M + \text{Na}$ ], 388.0073, found 411.1373.

#### Synthesis of 2,6-diiodo-BODIPY (**2**)

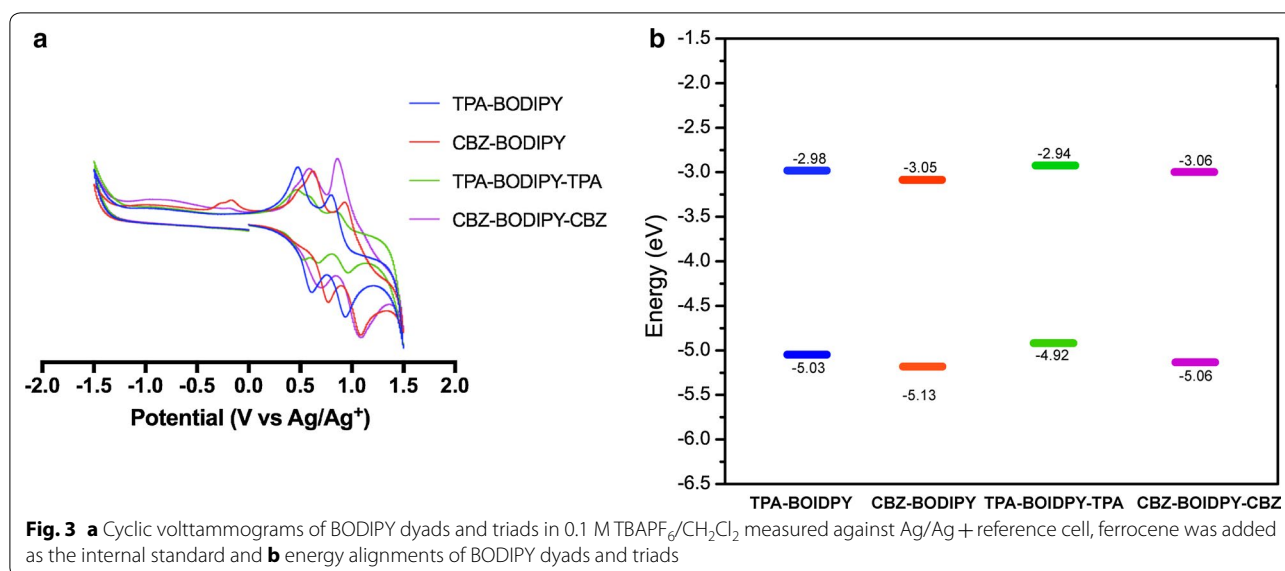
BODIPY precursor (0.35 g, 1.3 mmol) was dissolved in chloroform (20 mL) and the reaction mixture was degassed for 10 min. A solution of NIS (0.74 g, 3.3 mmol) in anhydrous DMF (5 mL) was slowly added to a solution mixture. The reaction mixture was stirred at room temperature for 2 days. After that, the crude mixture was

**Table 1** Photophysical and electrochemical properties of BODIPY dyads and triads

Compounds	$\lambda_{\text{max}}$ (nm)	$\epsilon_{\text{max}}$ ( $\times 10^4$ $\text{M}^{-1} \text{cm}^{-1}$ )	$\lambda_{\text{onset}}$ (nm)	$E_{\text{gr, opt}}$ (eV)	$E_{\text{ox}}$ (V)	HOMO <sup>a</sup> (eV)	LUMO <sup>b</sup> (eV)
TPA-BODIPY	307, 512	2.1, 4.3	605	2.05	+0.39	−5.03	−2.98
CBZ-BODIPY	269, 511	4.5, 7.9	599	2.07	+0.45	−5.13	−3.05
TPA-BODIPY-TPA	291, 537	4.3, 3.6	625	1.98	+0.23	−4.92	−2.94
CBZ-BODIPY-CBZ	270, 531	8.3, 8.3	619	2.00	+0.37	−5.06	−3.06

<sup>a</sup> HOMO energy is calculated from the equation,  $\text{HOMO} = -(E_{\text{ox}} + 4.8)$  [23]

<sup>b</sup> LUMO energy is calculated from the equation,  $E_{\text{gr, opt}} = \text{LUMO} - \text{HOMO}$



extracted with ethyl acetate and water. The organic layers were dried over Na<sub>2</sub>SO<sub>4</sub> and concentrated using a rotary evaporator. The crude mixture was then purified by column chromatography over silica with DCM/hexane as an eluent to give the product **2** as red powder (0.50 g, 74%). <sup>1</sup>H-NMR (500 MHz, CDCl<sub>3</sub>): δ (ppm), 2.62 (s, 6H, CH<sub>3</sub>), 2.53 (s, 3H, CH<sub>3</sub>), 2.46 (d, 6H, CH<sub>3</sub>) MALDI-TOF MS (*m/z*) calculated for C<sub>14</sub>H<sub>15</sub>BF<sub>2</sub>I<sub>2</sub>N<sub>2</sub>, 513.9386, found 513.9382.

#### Synthesis of TPA-BODIPY (**3**)

2-Iodo-BODIPY (0.37 g, 0.94 mmol) and triphenylamine-4-boronic acid (0.35 g, 1.2 mmol) were dissolved in toluene (15 mL). The mixture was degassed for 10 min. Then, Pd(PPh<sub>3</sub>)<sub>4</sub> (0.1 g, 0.09 mmol) and K<sub>2</sub>CO<sub>3</sub> (2 M) were added. The reaction mixture was stirred under reflux under N<sub>2</sub> atmosphere for 24 h. The reaction mixture was extracted with DCM and the organic layer was washed with water twice and dried over Na<sub>2</sub>SO<sub>4</sub>. The organic solvent was evaporated to dryness under reduced pressure. The residue was purified by column chromatography using DCM/hexane as the eluents to give **3** as an orange solid (0.3 g, 62%). <sup>1</sup>H-NMR (500 MHz, CDCl<sub>3</sub>): δ (ppm),

7.29–7.26 (m, 4H, CH<sub>AR</sub>), 7.17–7.11 (m, 6H, CH<sub>AR</sub>), 7.07–7.03 (m, 4H, CH<sub>AR</sub>) 6.07 (s, 1H, CH<sub>PR</sub>), 2.64 (s, 3H, CH<sub>3</sub>), 2.55–2.52 (d, 6H, CH<sub>3</sub>), 2.43 (s, 3H, CH<sub>3</sub>), 2.36 (s, 3H, CH<sub>3</sub>) <sup>13</sup>C-NMR (125 MHz, CDCl<sub>3</sub>): δ (ppm), 153.49, 152.54, 147.65, 146.77, 141.37, 140.77, 137.03 133.22, 131.05, 129.29, 127.42, 1124.55, 123.05, 123.02, 121.24, 17.37, 16.58, 15.50, 14.12, 13.34 MALDI-TOF MS (*m/z*) calculated for C<sub>32</sub>H<sub>30</sub>BF<sub>2</sub>NO<sub>3</sub> [M + Na], 528.2501, found 528.2523.

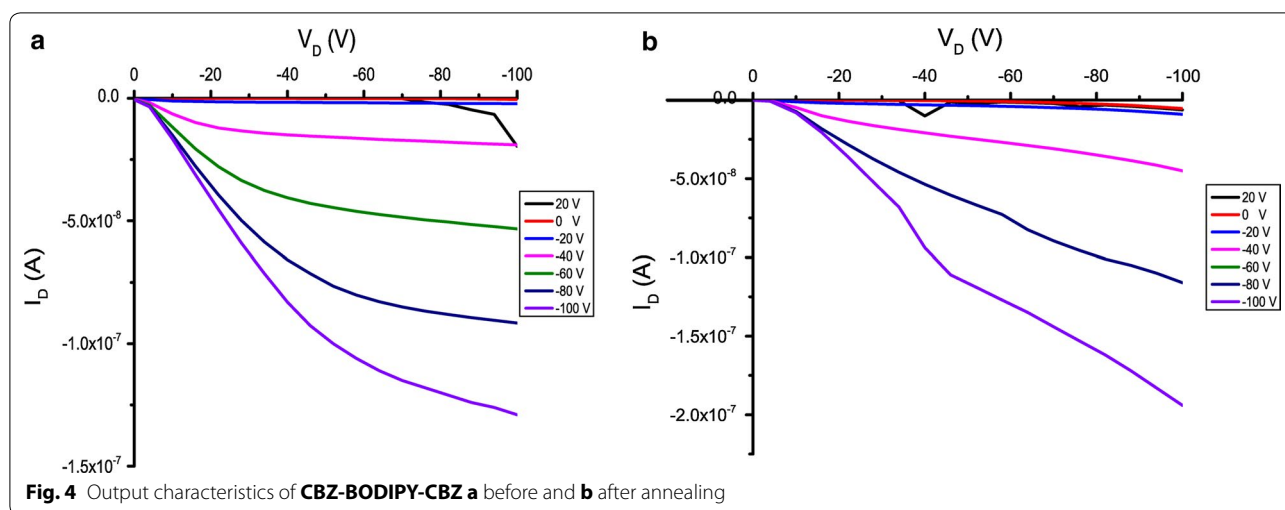
#### Synthesis of CBZ-BODIPY (**4**)

2-Iodo-BODIPY (0.13 g, 0.34 mmol) and 9-ethyl-carbazole-3-boronic acid (0.12 g, 0.51 mmol) were dissolved in toluene (15 mL) and degassed for 10 min. Then Pd(PPh<sub>3</sub>)<sub>4</sub> (0.04 g, 0.003 mmol) and K<sub>2</sub>CO<sub>3</sub> (2 M) were added. The reaction mixture was refluxed and stirred under N<sub>2</sub> for 24 h. The reaction mixture was extracted with DCM and the organic layer was washed with water twice and dried over Na<sub>2</sub>SO<sub>4</sub>. The organic solvent was evaporated to dryness under reduced pressure. The residue was purified by column chromatography using DCM/hexane as the eluents to yield the product **4** as an orange powder (0.10 g, 66%). <sup>1</sup>H-NMR (500 MHz, CDCl<sub>3</sub>): δ (ppm), 8.12

**Table 2** Organic thin-film transistor characteristics of BODIPY dyads and triads

Compounds	$\mu_h$ (cm <sup>2</sup> V <sup>-1</sup> s <sup>-1</sup> ) before annealing	$\mu_h$ (cm <sup>2</sup> V <sup>-1</sup> s <sup>-1</sup> ) after annealing	V <sub>T</sub> <sup>a</sup> (V)	I <sub>on</sub> /I <sub>off</sub> <sup>a</sup>
TPA-BODIPY	9.27 × 10 <sup>-7</sup>	1.55 × 10 <sup>-5</sup>	23	7.3
CBZ-BODIPY	5.29 × 10 <sup>-8</sup>	7.37 × 10 <sup>-7</sup>	69	5.6
TPA-BODIPY-TPA	1.66 × 10 <sup>-6</sup>	5.10 × 10 <sup>-8</sup>	42	10 <sup>2</sup>
CBZ-BODIPY-CBZ	7.86 × 10 <sup>-6</sup>	2.95 × 10 <sup>-5</sup>	52	10 <sup>2</sup>

<sup>a</sup> Before annealing



(d,  $J = 7.5$  Hz, 1H,  $\text{CH}_{\text{AR}}$ ), 7.94 (s, 1H,  $\text{CH}_{\text{AR}}$ ), 7.51–7.44 (m, 4H,  $\text{CH}_{\text{AR}}$ ), 7.31 (m, 1H,  $\text{CH}_{\text{AR}}$ ), 7.27 (m, 1H,  $\text{CH}_{\text{AR}}$ ), 6.09 (s, 1H,  $\text{CH}_{\text{PYR}}$ ), 4.44 (q, 2H,  $\text{CH}_2$ ), 2.65 (s, 3H,  $\text{CH}_3$ ), 2.58–2.56 (d, 6H,  $\text{CH}_3$ ), 2.44 (s, 3H,  $\text{CH}_3$ ), 2.37 (s, 3H,  $\text{CH}_3$ ), 1.48 (t, 3H,  $\text{CH}_3$ )  $^{13}\text{C}$ -NMR (125 MHz,  $\text{CDCl}_3$ ):  $\delta$  (ppm), 153.14, 141.33, 140.46, 140.21, 139.08, 137.46, 134.54, 132.19, 132.00, 128.01, 125.83, 124.03, 123.00, 122.70, 122.09, 121.04, 120.40, 118.93, 108.54, 37.59, 17.32, 16.72, 15.51, 14.41, 13.84, 13.37 MALDI-TOF MS ( $m/z$ ) calculated for  $\text{C}_{28}\text{H}_{28}\text{BF}_2\text{N}_3$  [ $M + \text{Na}$ ], 455.2344; found 478.224.

#### Synthesis of TPA-BODIPY-TPA (5)

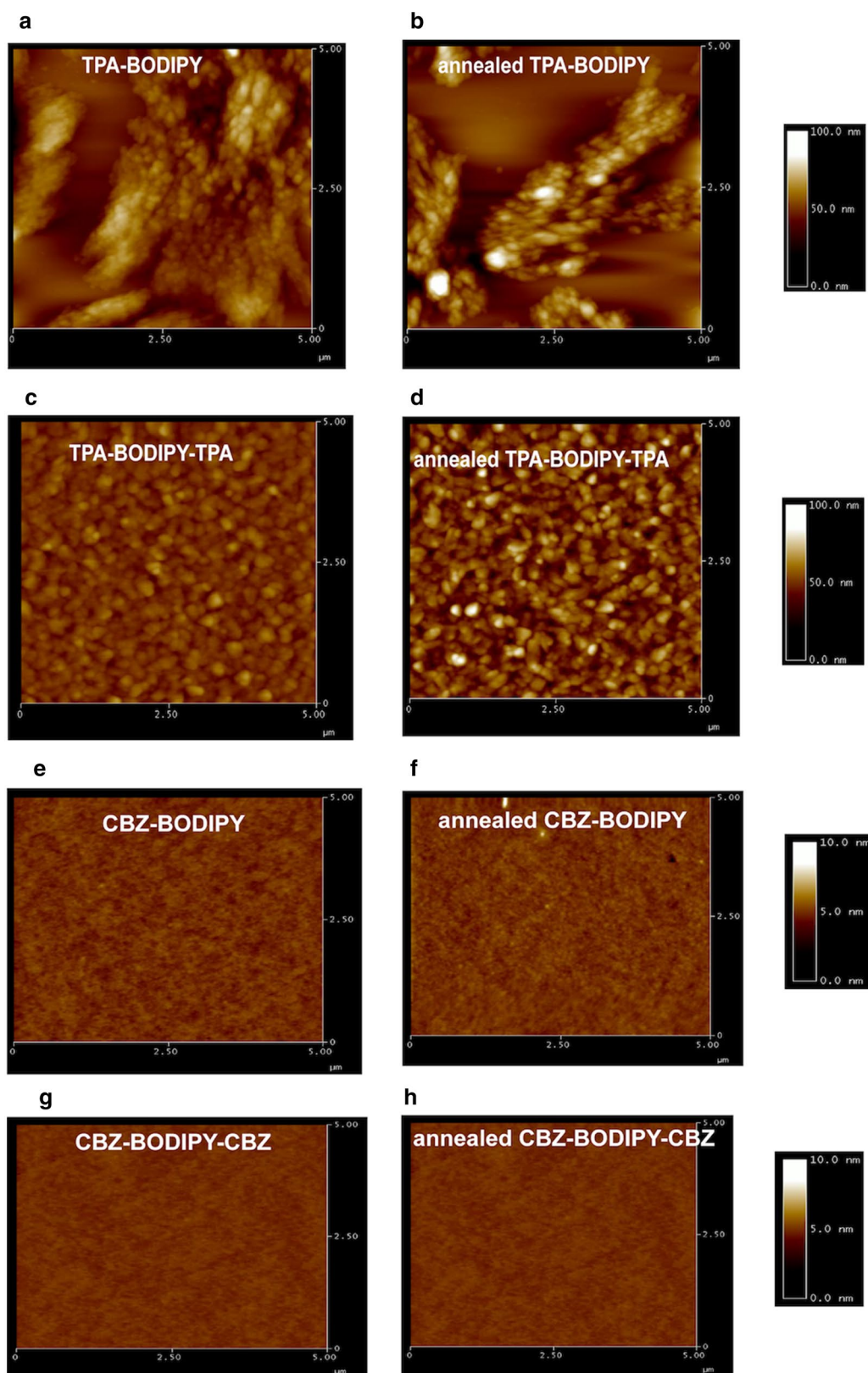
2,6-Diiodo-BODIPY (**2**) (0.20 g, 0.39 mmol) and triphenylamine-4-boronic acid (0.33 g, 1.1 mmol) were dissolved in toluene (15 mL). The solution was purged with nitrogen gas for 10 min. Then,  $\text{Pd}(\text{PPh}_3)_4$  (0.07 g, 0.06 mmol) and  $\text{K}_2\text{CO}_3$  (2 M) were added. The reaction mixture was stirred and refluxed for 48 h. After completion of the reaction, the mixture was cooled to room temperature, followed by extraction with DCM and water. The organic layers were dried over  $\text{Na}_2\text{SO}_4$  and concentrated in vacuo. The crude mixture was then purified by column chromatography using DCM/hexane as the eluents to yield **5** (0.17 g, 58%) purple solid.  $^1\text{H}$ -NMR (500 MHz,  $\text{CDCl}_3$ ):  $\delta$  (ppm), 7.30–7.27 (m, 8H,  $\text{CH}_{\text{AR}}$ ), 7.17–7.12 (m, 12H,  $\text{CH}_{\text{AR}}$ ), 7.09–7.03 (m, 8H,  $\text{CH}_{\text{AR}}$ ), 2.72 (s, 3H,  $\text{CH}_3$ ), 2.55 (s, 6H,  $\text{CH}_3$ ), 2.37 (s, 6H,  $\text{CH}_3$ )  $^{13}\text{C}$ -NMR (125 MHz,  $\text{CDCl}_3$ ):  $\delta$  (ppm), 152.47, 147.67, 146.79, 141.29, 136.74, 133.25, 132.25, 131.09, 129.30, 127.47, 124.57, 123.07, 122.03, 17.27, 15.61, 13.38 HRMS (MALDI-TOF MS) ( $m/z$ ) calculated for  $\text{C}_{50}\text{H}_{43}\text{BF}_2\text{N}_4$ , 748.3549; found 748.3662.

#### Synthesis of CBZ-BODIPY-CBZ (6)

2,6-Diiodo-BODIPY (**2**) (0.20 g, 0.4 mmol) and 9-ethyl-carbazole-3-boronic acid (0.26 g, 1 mmol) were dissolved in toluene (15 mL). The solution was degassed for 10 min. Next,  $\text{Pd}(\text{PPh}_3)_4$  (0.07 g, 0.06 mmol) and  $\text{K}_2\text{CO}_3$  (2 M) were added. After which, the reaction mixture was stirred under reflux for 48 h. The crude mixture was extracted with EtOAc and water. The organic layers were dried over  $\text{Na}_2\text{SO}_4$  and concentrated under reduced pressure. The crude product was then purified by column chromatography using DCM/hexane as the eluents to provide **6** as maroon solid (0.16 g, 64%).  $^1\text{H}$ -NMR (500 MHz,  $\text{CDCl}_3$ ):  $\delta$  (ppm), 8.16 (d,  $J = 7.5$  Hz, 1H,  $\text{CH}_{\text{AR}}$ ), 8.00 (s, 1H,  $\text{CH}_{\text{AR}}$ ), 7.55–7.47 (m, 6H,  $\text{CH}_{\text{AR}}$ ), 7.38 (d, 2H,  $\text{CH}_{\text{AR}}$ ), 7.36–7.27 (m, 2H,  $\text{CH}_{\text{AR}}$ ), 4.47 (q, 4H,  $\text{CH}_2$ ), 2.79 (s, 3H,  $\text{CH}_3$ ), 2.61 (d, 6H,  $\text{CH}_3$ ), 2.45 (s, 6H,  $\text{CH}_3$ ), 1.54 (t, 3H,  $\text{CH}_3$ )  $^{13}\text{C}$ -NMR (125 MHz,  $\text{CDCl}_3$ ):  $\delta$  (ppm), 152.68, 141.21, 140.25, 139.11, 137.02, 134.41, 132.21, 132.21, 128.11, 125.84, 124.22, 123.03, 122.77, 122.18, 121.45, 118.95, 108.56, 108.30, 37.65, 17.22, 15.63, 13.88, 13.41 HRMS (MALDI-TOF MS) ( $m/z$ ) calculated for  $\text{C}_{42}\text{H}_{39}\text{BF}_2\text{N}_4$  [ $M + \text{Na}$ ], 671.3236; found. 671.4772.

#### Instrumentations

$^1\text{H}$ -NMR spectra were recorded on 400 and 500 MHz Bruker NMR spectrometer and were reported in ppm using the solvents as the internal standard ( $\text{CDCl}_3$  at 7.26 ppm).  $^{13}\text{C}$ -NMR spectra were proton decoupled and recorded on a 100 MHz Bruker spectrometer using the carbon signal of the deuterated solvent as the internal standard. The exact mass measurements were recorded on Bruker Daltonics micrOTOF mass spectrometer. UV–vis absorption spectra were recorded on a Thermo Scientific UV-Genesys 10 s spectrophotometer. Electrochemical measurements were performed on a BASI

**Fig. 5** AFM topographic images

Epsilon potentiostat. Charge carrier mobility was determined in field effect transistor (FET) mode using Agilent 4165C precision semiconductor parameter analyzer. Surface morphology of BODIPY films were characterized using a digital instrument dimension 3100 atomic force microscope (AFM). The cantilever specifications are described as follows: spring constant of 40 N/m, resonance frequency of 300 kHz, tip radius of 8 nm.

### FET fabrication

Bottom contacted field effect transistor (FET) devices were fabricated following our previous procedure [23]. Briefly, the BODIPYs (3–6), concentration of 10 mg/mL in dichlorobenzene, were deposited on the FET substrate using a spin coater. All mobility measurements were performed in a glove box under argon atmosphere at a temperature of 25 °C. Thermal annealing was done in glove box under argon atmosphere. Briefly, a hot plate was preheated to 80 °C. Then, FET devices were placed on the hot plate and they were heated directly at the constant temperature for 3 h. After that, the devices were removed from the hot plate and allowed to cool down to room temperature and the mobilities were measured again.

### Additional file

**Additional file 1.** NMR spectroscopic data, FET and AFM measurements of BODIPY dyads and triads.

### Authors' contributions

SW designed and synthesized all BODIPY derivatives and characterized chemical structures using <sup>1</sup>H-NMR, <sup>13</sup>C-NMR and MS, performed UV-Vis spectrometry and OFET experiment and collect data. PK performed cyclic voltammetry, OFET, and AFM measurements and collect data. SW, PK and ST analyze data and wrote paper. All authors read and approved the final manuscript.

### Author details

<sup>1</sup> Polymer for Energy, Environment and Technology Research Group, Division of Materials Technology, School of Energy, Environment and Materials, King Mongkut's University of Technology Thonburi, 126 Pracha Uthit Rd., Bang Mod, Thung Khru, Bangkok 10140, Thailand. <sup>2</sup> Nanotec-KMUTT Center of Excellence on Hybrid Nanomaterials for Alternative Energy, King Mongkut's University of Technology Thonburi, 126 Pracha Uthit Rd., Bang Mod, Thung Khru, Bangkok 10140, Thailand. <sup>3</sup> Department of Chemistry, University of Massachusetts Amherst, Amherst 10300, USA.

### Acknowledgements

This study was funded by Thailand Research Fund (Grant no. TRG5880211) to Dr. Sompit Wanwong. Partial funding provided by the National Nanotechnology Center (NANOTEC), NSTDA, Ministry of Science and Technology, through its program of Center of Excellence Network Thailand is acknowledged. This work was also partially supported by the US Army Research Office (W911NF-15-1-0568) to Prof. Sankaran Thayumanavan.

### Competing interests

The authors declare that they have no competing interests.

### Availability of data and materials

With the authors.

### Consent of publication

Not applicable.

### Ethics approval and consent to participate

Not applicable.

### Publisher's Note

Springer Nature remains neutral with regard to jurisdictional claims in published maps and institutional affiliations.

Received: 2 December 2017 Accepted: 4 May 2018

Published online: 11 May 2018

### References

1. Clarke TM, Durrant JR (2010) Charge photogeneration in organic solar cells. *Chem Rev* 110:6736–6767
2. Mazzi KA, Luscombe CK (2015) The future of organic photovoltaics. *Chem Soc Rev* 44:78–90
3. Lu LY, Zheng TY, Wu QH, Schneider AM, Zhao DL, Yu LP (2015) Recent advances in bulk heterojunction polymer solar cells. *Chem Rev* 115:12666–12731
4. Wang Q, Xie Y, Soltani-Kordshuli F, Eslamian M (2016) Progress in emerging solution-processed thin film solar cells—part I: polymer solar cells. *Renew Sustain Energy Rev* 56:347–361
5. Machui F, Hosel M, Li N et al (2014) Cost analysis of roll-to-roll fabricated ITO free single and tandem organic solar modules based on data from manufacture. *Energy Environ Sci* 7:2792–2802
6. Mishra A, Bauerle P (2012) Small molecule organic semiconductors on the move: promises for future solar energy technology. *Angew Chem Int Ed* 51:2020–2067
7. Lin YZ, Li YF, Zhan XW (2012) Small molecule semiconductors for high-efficiency organic photovoltaics. *Chem Soc Rev* 41:4245–4272
8. Liu CL, Chen Y, Shelar DP, Li C, Cheng G, Fu WF (2014) Bodipy dyes bearing oligo(ethylene glycol) groups on the meso-phenyl ring: tuneable solid-state photoluminescence and highly efficient OLEDs. *J Mater Chem C* 2:5471–5478
9. Squeo BM, Gregoriou VG, Ayeropoulos A et al (2017) BODIPY-based polymeric dyes as emerging horizon materials for biological sensing and organic electronic applications. *Prog Polym Sci* 71:26–52
10. Singh SP, Gayathri T (2014) Evolution of BODIPY dyes as potential sensitizers for dye-sensitized solar cells. *Eur J Org Chem* 2014(22):4689–4707
11. Bessette A, Hanan GS (2014) Design, synthesis and photophysical studies of dipyrromethene-based materials: insights into their applications in organic photovoltaic devices. *Chem Soc Rev* 43:3342–3405
12. Chen JJ, Conron SM, Erwin P, Dimitriou M, McAlahney K, Thompson ME (2015) High-efficiency BODIPY-based organic photovoltaics. *ACS Appl Mater Interfaces* 7:662–669
13. Lu H, Mack J, Yang YC, Shen Z (2014) Structural modification strategies for the rational design of red/NIR region BODIPYs. *Chem Soc Rev* 43:4778–4823
14. Wanwong S, Surawatanawong P, Khumsubdee S, Kanchanakungwankul S, Wootthikanokkhan J (2016) Synthesis, optical, and electrochemical properties, and theoretical calculations of BODIPY containing triphenylamine. *Heteroatom Chem* 27:306–315
15. Sengupta S, Pandey UK, Athresh EU (2016) Regioisomeric donor–acceptor–donor triads based on benzodithiophene and BODIPY with distinct optical properties and mobilities. *RSC Adv* 6:73645–73649
16. Hendel SJ, Poe AM, Khomein P, Bae Y, Thayumanavan S, Young ER (2016) Photophysical and electrochemical characterization of BODIPY-containing dyads comparing the influence of an A–D–A versus D–A motif on excited-state photophysics. *J Phys Chem A* 120:8794–8803
17. Singh S, Venugopalan V, Krishnamoorthy K (2014) Organic soluble and uniform film forming oligoethylene glycol substituted BODIPY small molecules with improved hole mobility. *Phys Chem Chem Phys* 16:13376–13382
18. Poe AM, Della Pelle AM, Subrahmanyam AV, White W, Wantz G, Thayumanavan S (2014) Small molecule BODIPY dyes as non-fullerene



- acceptors in bulk heterojunction organic photovoltaics. *Chem Commun* 50:2913–2915
19. Ozdemir M, Choi D, Kwon G et al (2016) Solution-processable BODIPY-based small molecules for semiconducting microfibers in organic thin-film transistors. *ACS Appl Mater Interfaces* 8:14077–14087
  20. Ning ZJ, Tian H (2009) Triarylamine: a promising core unit for efficient photovoltaic materials. *Chem Commun* 2009(37):5483–5495
  21. Sathiyam G, Sivakumar EKT, Ganesamoorthy R, Thangamuthu R, Sakthivel P (2016) Review of carbazole based conjugated molecules for highly efficient organic solar cell application. *Tetrahedron Lett* 57:243–252
  22. Sasaki S, Drummen GPC, Konishi G (2016) Recent advances in twisted intramolecular charge transfer (TICT) fluorescence and related phenomena in materials chemistry. *J Mater Chem C* 4:2731–2743
  23. Wanwong S, Poe A, Balaji G, Thayumanavan S (2014) The effect of heteroatom conformation on optoelectronic properties of cyclopentadithiophene derivatives. *Org Biomol Chem* 12:2474–2478
  24. Mas-Torrent M, Rovira C (2008) Novel small molecules for organic field-effect transistors: towards processability and high performance. *Chem Soc Rev* 37:827–838
  25. Wang CL, Dong HL, Hu WP, Liu YQ, Zhu DB (2012) Semiconducting pi-conjugated systems in field-effect transistors: a material odyssey of organic electronics. *Chem Rev* 112:2208–2267
  26. Galindo S, Tamayo A, Leonardi F, Mas-Torrent M (2017) Control of polymorphism and morphology in solution sheared organic field-effect transistors. *Adv Funct Mater*. <https://doi.org/10.1002/adfm.201700526>
  27. Coropceanu V, Cornil J, da Silva DA, Olivier Y, Silbey R, Bredas JL (2007) Charge transport in organic semiconductors. *Chem Rev* 107:926–952
  28. Murphy AR, Frechet MJM (2007) Organic semiconducting oligomers for use in thin film transistors. *Chem Rev* 107:1066–1096

Submit your manuscript to a SpringerOpen<sup>®</sup> journal and benefit from:

- Convenient online submission
- Rigorous peer review
- Open access: articles freely available online
- High visibility within the field
- Retaining the copyright to your article

---

Submit your next manuscript at ► [springeropen.com](http://springeropen.com)

---